Article

Electronic Expansion Valve Experimental System Debugging Solution Based on PI Control Algorithm on Single-Tube Heat Exchange Experimental Platform

Jinfeng Wang [1,2,3,4] , Wanying Chang [1] and Jing Xie [1,2,3,4,*]

1   College of Food Science and Technology, Shanghai Ocean University, Shanghai 201306, China; jfwang@shou.edu.cn (J.W.); m180310731@st.shou.edu.cn (W.C.)
2   Shanghai Professional Technology Service Platform on Cold Chain Equipment Performance and Energy Saving Evaluation, Shanghai 201306, China
3   Shanghai Engineering Research Center of Aquatic Product Processing & Preservation, Shanghai 201306, China
4   National Experimental Teaching Demonstration Center for Food Science and Engineering, Shanghai Ocean University, Shanghai 201306, China
*   Correspondence: jxie@shou.edu.cn; Tel.: +86-02161900391

Abstract: In this paper, the electronic expansion valve (EXV) on the single-tube heat exchange experimental platform was used as a research object. Firstly, the EXVs were selected according to the experimental requirements, and the functional parameters were set. Subsequently, the effective opening ranges of the EXVs were determined by manual control, and the control effects of the EXVs installed at the front and back ends of the test section were compared. Finally, by self-tuning and optimizing the best response curves, the proportional and integral coefficients suitable for the experimental platform were obtained; thus, the automatic intelligent control of EXV based on the proportional integral (PI) control algorithm was realized. From setting EXV functional parameters to realizing PI control, an appropriate experimental system-debugging solution for the whole process could be obtained. Based on the solution, the system stability could be improved, and the transition process time could be shortened. Furthermore, the solution also provided a method to guarantee the accuracy of experimental data and could be applied to the debugging of similar experimental systems.

Keywords: PI control algorithm; EXV opening; self-tuning; response curve; experimental platform

1. Introduction

The electronic expansion valve (EXV) is widely used for its flexible control, rapid response, and relatively independent sensing, adjustment, and execution components [1–3]. Typically, the EXV is mostly used to regulate the flow rate of the refrigerants [4–8], and the influence of various factors on the flow rate characteristics of the EXV have been frequently studied [9,10]. Knabben et al. [11] studied the flow characteristics of EXV in a household refrigeration application and proposed a model to predict the mass flow of EXV. Liu et al. [12] investigated the effects of inlet pressure and temperature and EXV opening on the flow characteristics of CO_2 through the EXV and predicted the mass flow rate through the EXV, and the results showed that the maximum deviation of the predicted value was less than 15.3%. Chen et al. [13] showed that the mass flow rate of R245fa refrigerant increases with increasing openness, condensing temperature, subcooling, and orifice diameter, as it flows through the EXV.

In addition, more and more scholars are studying EXV because of its wide range of regulations and the possibility of controlling them by combining frequency conversion technology and intelligent control [14–18]. Xia et al. [19] investigated the effect of the EXV characteristics of proportional integral (PI) control on the stability of refrigeration systems, and the results showed that smaller proportional and integral coefficients and slower temperature transfer contribute to system stability. Ding [20] has developed an

online self-tuning PI algorithm for controlling EXV, which improves the heat transfer efficiency of the evaporator. In the case of objects with smaller time constants, such as boiler steam superheaters or other heat exchangers [21], Dawid Taler presented the medium temperature monitoring system based on digital PID controller to control at the exchanger will be much higher. Al-Badri [22] studied the control effect of the PI control algorithm for EXV, and compared it with proportional integral derivative and proportional fuzzy algorithms. Dawid Taler [23] proposed a digital PID controller to maintain a constant hot water temperature in the tank, which is the determination of the fluid temperature based on the solution of the inverse problem of heat conduction formulated for a thermometer. Moreover, it was found that combining the algorithms with different control methods can improve the performance and stability of the system.

Regarding the single-tube heat exchange experimental platform, it can study the heat exchange characteristics of different refrigerants in the tubes, the flow state of the refrigerants in the tubes, and the switching of various tube types [24–27]. Therefore, more and more scholars have started to build heat transfer experimental platforms to investigate the heat transfer characteristics of different refrigerants and different tube types [28–31].

However, the current research focuses on the application of EXV, and the function parameters setting of EXV, while the determination of its effective opening range is rarely mentioned or studied, and the EXV in the experimental platform is generally located at a fixed position in the refrigerant circulation circuit, and the control effects of EXVs in different positions are rarely compared. Moreover, the control of EXV on the experimental platform is generally manual and cumbersome, and relatively few reference data are provided in the processes of experiment and debugging. Therefore, in this paper, the same type of EXVs was selected for installation at the front and end of the test section. By setting the EXV functional parameters and determining its effective opening range, it can achieve reasonable control of the degree of superheat (DS) at the outlet of the test section. It also realizes the control of EXV by the PI control algorithm through self-tuning and self-tuning optimization.

2. EXV Setting

2.1. Experimental Platform with EXV

The system schematic diagram of the single-tube heat exchange experimental platform is shown in Figure 1 [32]. In the design calculation stage for the experimental platform, the refrigerant flow rate ranges from 0.565 to 112.176 kg/h, the refrigerant heat exchange rate ranges from 0.031 to 6.232 kW, the water flow rate ranges from 0.006 to 3.911 m^3/h, and the design pressure of the tube is 3.455 MPa [33].Therefore, the experimental platform uses the pressure sensor with a range of 0 to 4 MPa, the mass flow meter with ranges of 0 to 0.6 kg/min and 0 to 5 kg/min, and the electromagnetic flow meter with a range of 0 to 6.3 m^3/h to collect experimental data [33]. Additionally, as shown in Figure 1, EXVs are installed at both the front and rear ends of the test section, and a bypass circuit is connected in parallel near the EXV to test the control effect of the EXV at different positions on the DS of the test section outlet. The EXV used in the platform is Danfoss ETS 6 type electric expansion valve, which is small in size, light in weight, and compact in structure; it is suitable for R22, R410A, R134a, and other common refrigerants, which can meet different experimental requirements while ensuring the energy efficiency of the system [34].

The expansion valve has a stepper motor of type ETS 6. As shown in Figure 2, different winding configurations exist inside its coil structure, and the polarities are changed by the electrical signals applied. When the coil is energized, the appropriate combination of signals is applied in the form of pulses, and the coil directly drives the valve rotor step. The DS of the test section is determined by the outlet temperature and pressure of the test section, and the collected temperature and pressure signals are transmitted to the controller through the sensor. Subsequently, the electric pulse actuation signal is output to the stepper motor following its inner loop control and the linear motion of the screw mechanism, thus controlling the opening of the EXV.
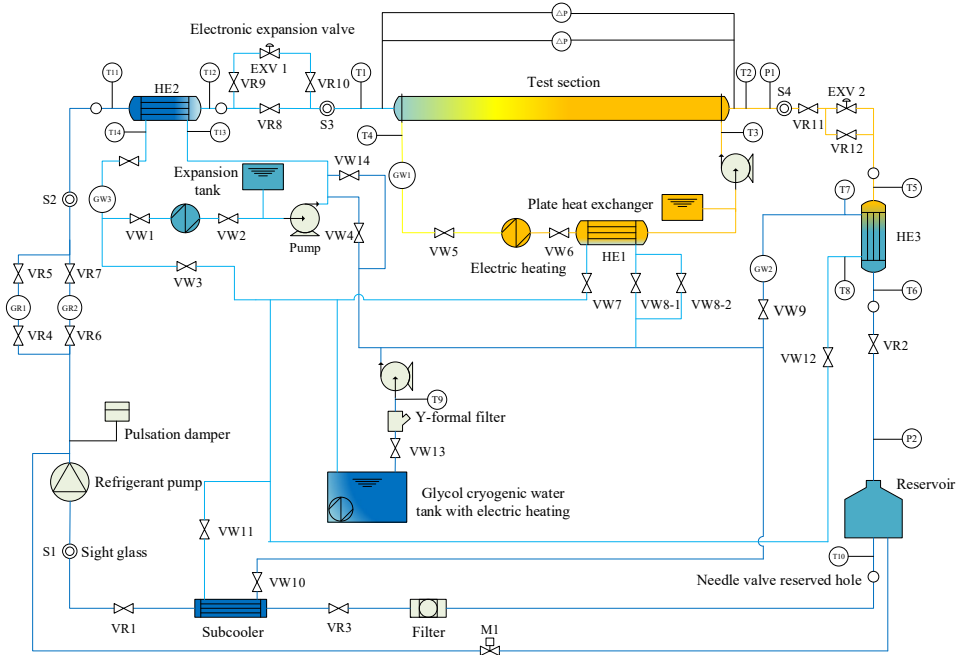
Figure 1. System schematic diagram of the single-tube heat exchange experimental platform [32].
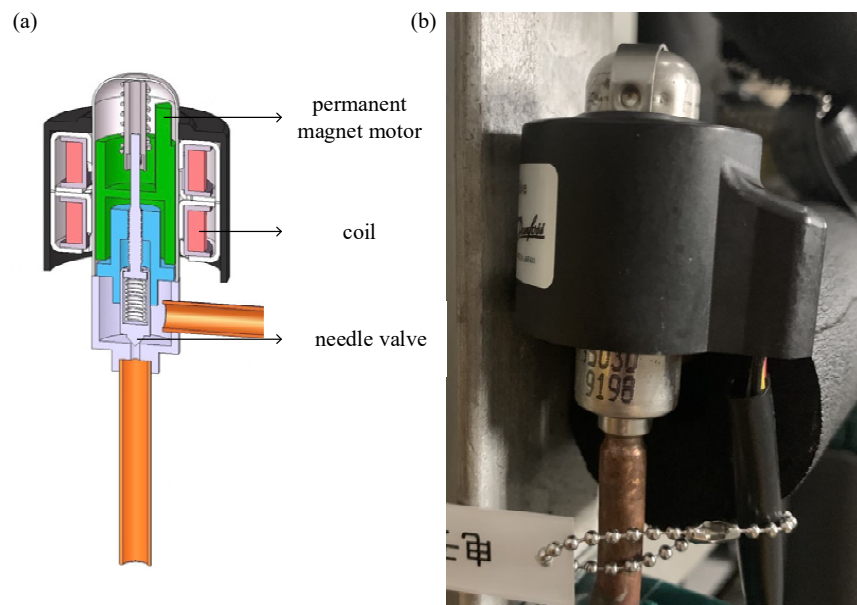

Figure 2. ETS 6 type EXV (**a**) cross-sectional view [34]; (**b**) physical image.

2.2. EXV Settings

Manual control is used to control the refrigerant pump frequencies and the opening of the EXV to study the system performance and characteristics under different operating conditions, thereby further improving the EXV settings. The DS control range is determined by setting the EXV opening at the maximum value and then gradually decreasing it to find the maximum and minimum value of the DS during stable operation of the system [22]. As can be seen from Table 1, the DS control range is 4–10 °C.

Table 1. EXV opening and corresponding DS at three refrigerant pump frequencies.

T3 (°C)	T7 (°C)	Refrigerant Pump Frequencies (Hz)		
		15	17.5	20
		EXV Opening (%)/DS (°C)		
21	−5	25/6.91	15/5.86	10/4.11
22	−5	30/8.13	20/7.11	13/6.03
23	−5	65/9.91	60/9.15	30/8.51

For the experimental platform, the EXV settings are shown in Table 2. In the evaporative heat exchange experiment, the selected refrigerant is R22, and the set value of refrigerant type is 2. The pressure sensor range is 0–5 kg/min, and the controller is controlled by an external analog signal of 4–20 mA; the set value is 2. The DS fluctuates within a limited range when the single-loop control method is used, indicating that the system has the best performance with the method [22]. Therefore, the set value of the control type is 1. In addition, when changing the functional parameters of the controller, we first set r12 to the OFF in the setting interface to turn off the controller.

Table 2. Settings of EXV.

Functional Parameters Name	Functional Parameters	Set Values
EXV model	n03	6
DS upper limit	n09	10 K
DS lower limit	n10	4 K
pressure sensor lower limit	o20	0 bar
pressure sensor upper limit	o21	5 bar
refrigerant type	030	2
manual control	o18	1
valve opening control	o45	0–100
external signal control	o61	1
signal type of external analog quantity	o10	2
control type	o56	1
max opening	n32	100%
number of steps from 0–100% opening	n37	262 stp
number of steps per second	n38	300 stp/s

When the settings are completed, we set r12 to the ON in the setting interface to turn on the controller. When the EXV is controlled by external analog or manually controlled, the EXV emits a short vibration sound to indicate that the target value is set.

3. Design of PI Control

3.1. Principle of DS Control

As shown in Figure 1, platinum resistors T1 and T2 are installed at the front and rear ends of the test section to collect their inlet and outlet temperatures. The calculated DS of the test section can be calculated from the difference between the two collected data sets. However, because the test section is too long, the refrigerant flow through the test section will generate a resistance pressure drop in practice. The larger the pressure drop, the larger the deviation of the calculated DS from the real DS. Therefore, to obtain a more accurate DS of the test section, the refrigerant saturation temperature corresponding to the pressure collected by the test section outlet pressure sensor P1 is used as the evaporation temperature T_e, and the difference is calculated with the temperature collected by the platinum resistor T2. The calculation formula is shown in Equation (1). Thus, more precise control of EXV can be obtained.

$$DS = T2 - T_e \tag{1}$$

The working range of ETS 6 EXV is 0–480 pulses. When P1 and T2 at the test section outlet feed the signal to the controller, the controller converts it into a real-time test section outlet DS signal and compares the target signal. The difference is then calculated and the flow rate through the EXV is adjusted according to the designed control logic, thus controlling the DS.

3.2. PI Control Algorithm

The regulating action of the proportional control responds quickly and contributes to the stability of the system, but there is still static deviation at the end of the regulation. The integral control can eliminate static deviations in the regulation process, but there are large fluctuations in the parameter being regulated and its regulation effect is slow to respond. Therefore, the PI control is used to control the EXV of the experimental platform by combining the characteristics of both, and its dynamic characteristic expression is shown in Equation (2).

$$u(t) = K_P \left[e(t) + \frac{1}{T_i} \int_0^t e(t)dt \right] \tag{2}$$

where: $u(t)$ is control algorithm output; $e(t)$ is control algorithm input; K_P is the proportional coefficient of the control algorithm; T_i is the integration time of the control algorithm.

To implement the PI control algorithm, Equation (2) needs to be discretized, as shown in Equation (3).

$$\int Edt = \sum_{j=0}^n Te(j) \tag{3}$$

Subsequently, Equation (3) is brought into Equation (2) to obtain the difference equation as shown in Equation (4).

$$u(n) = K_P \left[e(n) + \frac{T}{T_i} \sum_{j=0}^n e(j) \right] \tag{4}$$

where: n is the control serial number, $n = 0, 1, 2, 3 \ldots \ldots$, $u(n)$ is the control volume at the nth moment, $e(n)$ is the deviation value at the nth moment.

To reduce the occupation of the storage unit, an incremental PI control algorithm is used, as shown in Equation (5).

$$\Delta u(n) = u(n) - u(n-1) = K_P[e(n) - e(n-1)] + K_i e(n) \tag{5}$$

Subsequently, the response of the test section DS to EXV is approximated by a first-order transfer function with inertial delay, as shown in Equation (6) [35].

$$G(s) = k_1 e^{-s\tau} / (1 + T_1 s) \tag{6}$$

where $G(s)$ is the transfer function, k_1 is the test section gain, T_1 is the time constant, s is the Laplace operator, τ is the lag time.

Among them, the three parameters k_1, T_1, and τ depend on the operating conditions of the system, the size of the thermal load, and the configuration, and can be obtained from the impulse step response curve of the DS to the valve. Additionally, the Ziegler–Nichols [36] empirical formula can be used to tune the parameters, and the PI parameters self-tuning is shown in Table 3.

Table 3. PI parameters self-tuning [36].

Control Algorithm	Step Response Self-Tuning			Proportional Band
	K_p	T_i	T_d	
P	$1/\alpha$	∞	0	$\alpha = \frac{k_1 \tau}{T_1}$
PI	$0.9/\alpha$	3.3τ	0	

However, since the actual control effect of the initial parameter values rectified by the rectification method is not always optimal, adjustments are often required on this basis. Therefore, the dichotomous and bilinear interpolation methods can be used for self-tuning optimization.

4. Experiment and Analysis

To control the EXV on the experimental platform, the experimental system debugging solution has been established. Subsequently, experiments to determine the effective opening range, self-tuning and self-tuning optimization of PI control parameters, and implementation of PI control were conducted to verify the effectiveness and generalizability of the solution.

4.1. Determination of the Effective Opening Range of EXV1

Factors such as the frequency and opening of the refrigerant pump, the inlet refrigerant temperature in the test section, the inlet water temperature in the test section, and the inlet water temperature of the plate heat exchanger HE3 will all have a certain impact on the opening and self-tuning test data of the EXV1. Therefore, multiple sets of repetitive experiments should be carried out under different setting conditions to find a reasonable EXV1 opening range. To ensure single-phase entry and exit of the test section, the experimental conditions are shown in Table 4. Subsequently, the fluctuations in DS were observed by manually changing the EXV1 opening at refrigerant pump frequencies of 15 Hz, 17.5 Hz, and 20 Hz, respectively. It can be seen that the controlled variables in the experiment are the refrigerant pump opening and frequency, the inlet refrigerant temperature in the test section, the inlet water temperature in the test section, the inlet water temperature of the plate heat exchanger HE3, and the EXV1 opening, and the manipulated variable is the DS at the outlet of the test section.

Table 4. Experimental conditions.

Working Conditions	Refrigerant Pump Opening (%)	T1 °C	T3 °C	T7 °C	Refrigerant Pump Frequency (Hz)	EXV1 Opening (%)
1	40	2	23	−5		
2	60	0	32	−5	15, 17.5, 20	10–100
3	80	0	35	−5		

As shown in Figure 3, the change in DS at the outlet of the test section while changing the EXV1 opening from 100% to 40% under the condition of working condition 1 is not obvious, which indicates that the control effect of EXV1 on refrigerant is weak in the opening range. When the valve opening changes from 40% to 30%, the DS first decreases with time and then stabilizes, and the change is more obvious when the pump frequency is 15 Hz and 20 Hz. It may be because when the valve opening changes from 40% to 30%, the valve needle and the refrigerant inside the valve body go from a non-contact to contact process. During the period, certain air pressure will be generated, resulting in an increase in refrigerant flow and thereby a decrease in DS. When the EXV1 opening changes from 30% to 10%, the DS shows an obvious step response, and its value increases with time and then stabilizes. It proves that the EXV1 controls the refrigerant well in the opening range.

As can be seen from Figure 4, there is a small increase in DS but no significant step jump during changing the EXV1 opening from 100% to 30% in the condition of working condition 2. It shows that the EXV1 is not effective in controlling the refrigerant in the opening range. The change in DS when the EXV1 opening changes from 30% to 10% is similar to the situation when the refrigerant pump opening is 40%.
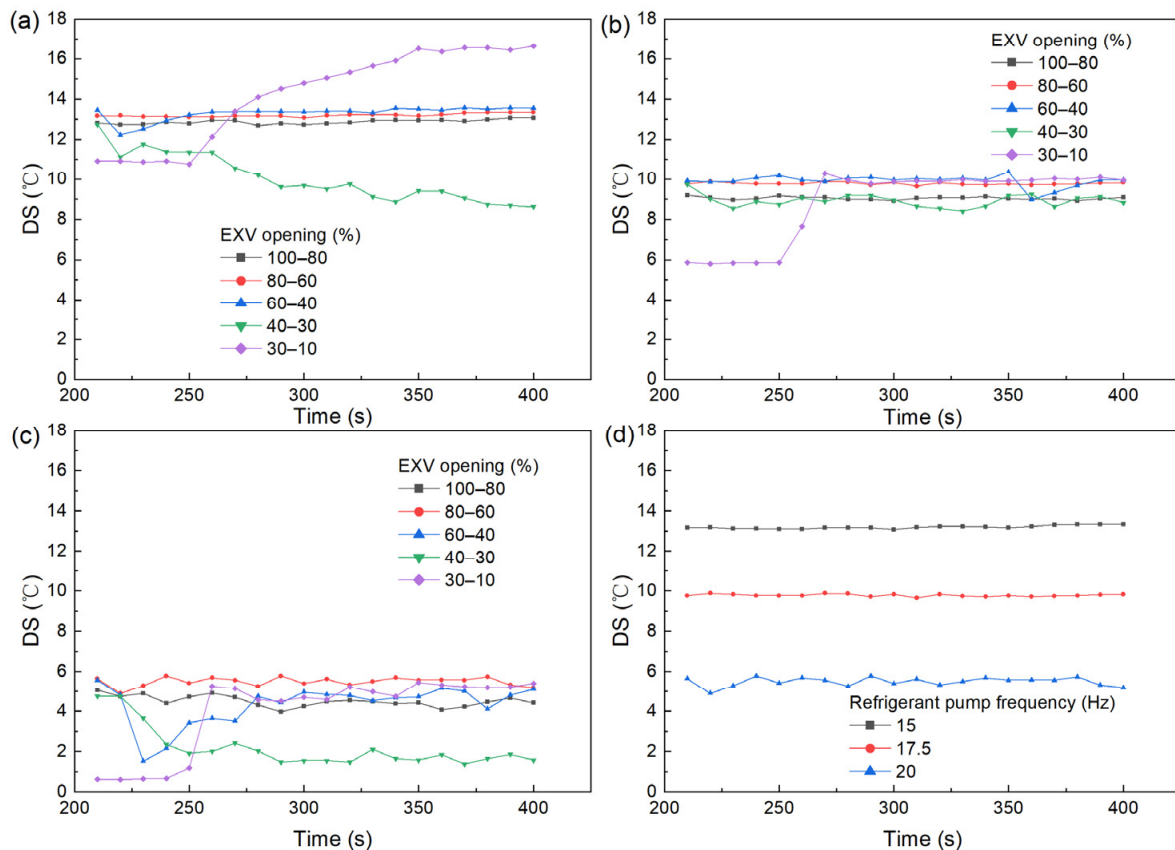
Figure 3. Change curves of DS when the refrigerant pump opening is 40% (**a**) the refrigerant pump frequency is 15 Hz, and the EXV1 opening is 100%–10%; (**b**) the refrigerant pump frequency is 17.5 Hz, and the EXV1 opening is 100%–10%; (**c**) the refrigerant pump frequency is 20 Hz, and the EXV1 opening is 100%–10%; (**d**) the EXV1 opening is 80%–60%, and the refrigerant pump frequency is 15 Hz, 17.5 Hz, and 20 Hz, respectively.

As can be seen from Figure 5, there is no significant step jump in the DS during changing the EXV1 opening from 100% to 30% under the condition of working condition 3 but its value fluctuates widely. It shows that the control effect of EXV on the refrigerant is not obvious in the opening range, but the opening of the refrigerant pump becomes larger, and the large flow rate causes the fluctuation of the value. The change in DS when the EXV1 opening changes from 30% to 10% is similar to the situation when the refrigerant pump opening is 40% and 60%.

Moreover, from Figures 3d, 4d and 5d, it can be seen that the DS decreases with the increase in the refrigerant pump frequency. This is because the mass flow rate of the refrigerant increases as the pump frequency increases, and it also shows the accuracy and rationality of the data collected by the experimental platform. In summary, it can be concluded that the best opening range for the EXV1 of the experimental platform is 10%–30%.

4.2. Self-Tuning

After the range of the EXV1 opening was determined, the change curves of DS with time during the process of the EXV1 opening from 30% to 10% when the refrigerant pump opening was 40%, 60%, and 80% were compared, as shown in Figure 6.
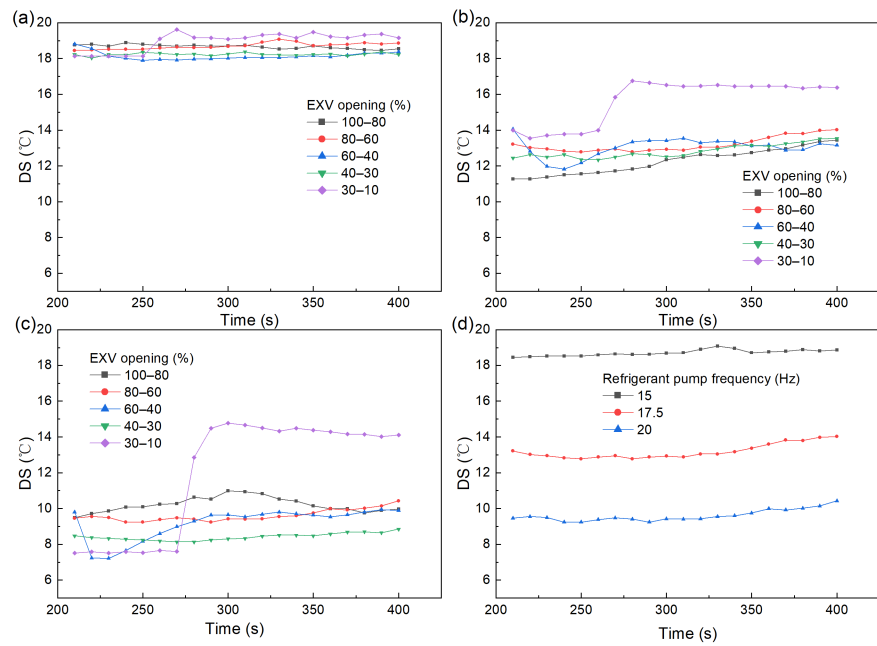
Figure 4. Change curves of DS when the refrigerant pump opening is 60% (**a**) the refrigerant pump frequency is 15 Hz, and the EXV1 opening is 100%–10%; (**b**) the refrigerant pump frequency is 17.5 Hz, and the EXV1 opening is 100%–10%; (**c**) the refrigerant pump frequency is 20 Hz, and the EXV1 opening is 100%–10%; (**d**) the EXV1 opening is 80%–60%, and the refrigerant pump frequency is 15 Hz, 17.5 Hz, and 20 Hz, respectively.
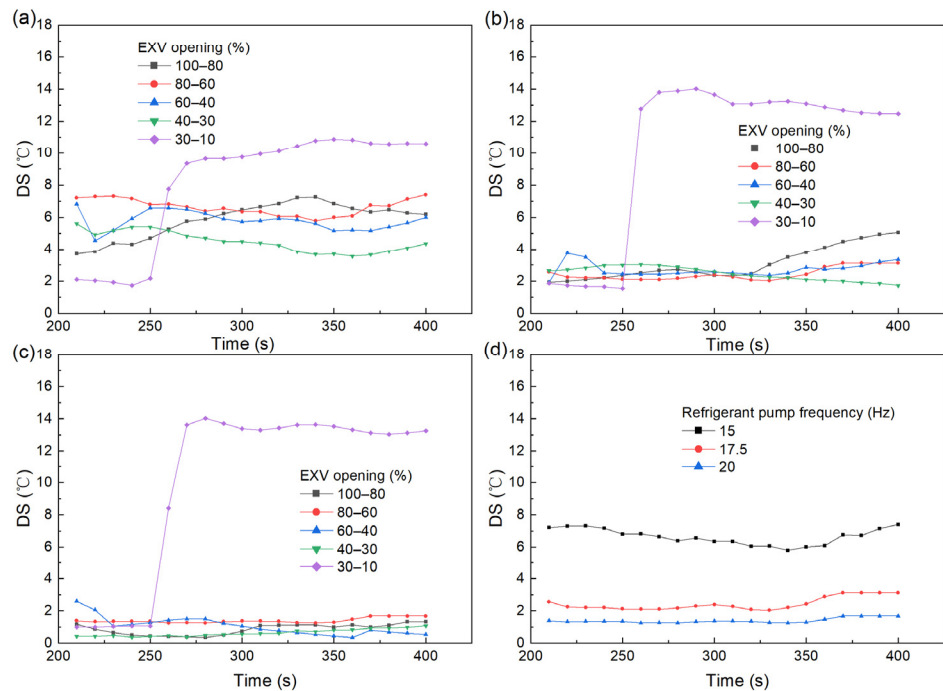

Figure 5. Change curves of DS when the refrigerant pump opening is 80% (**a**) the refrigerant pump frequency is 15 Hz, and the EXV1 opening is 100%–10%, (**b**) the refrigerant pump frequency is 17.5 Hz, and the EXV1 opening is 100%–10%, (**c**) the refrigerant pump frequency is 20 Hz, and the EXV1 opening is 100%–10%, (**d**) the EXV1 opening is 80%–60%, and the refrigerant pump frequency is 15 Hz, 17.5 Hz, and 20 Hz, respectively.
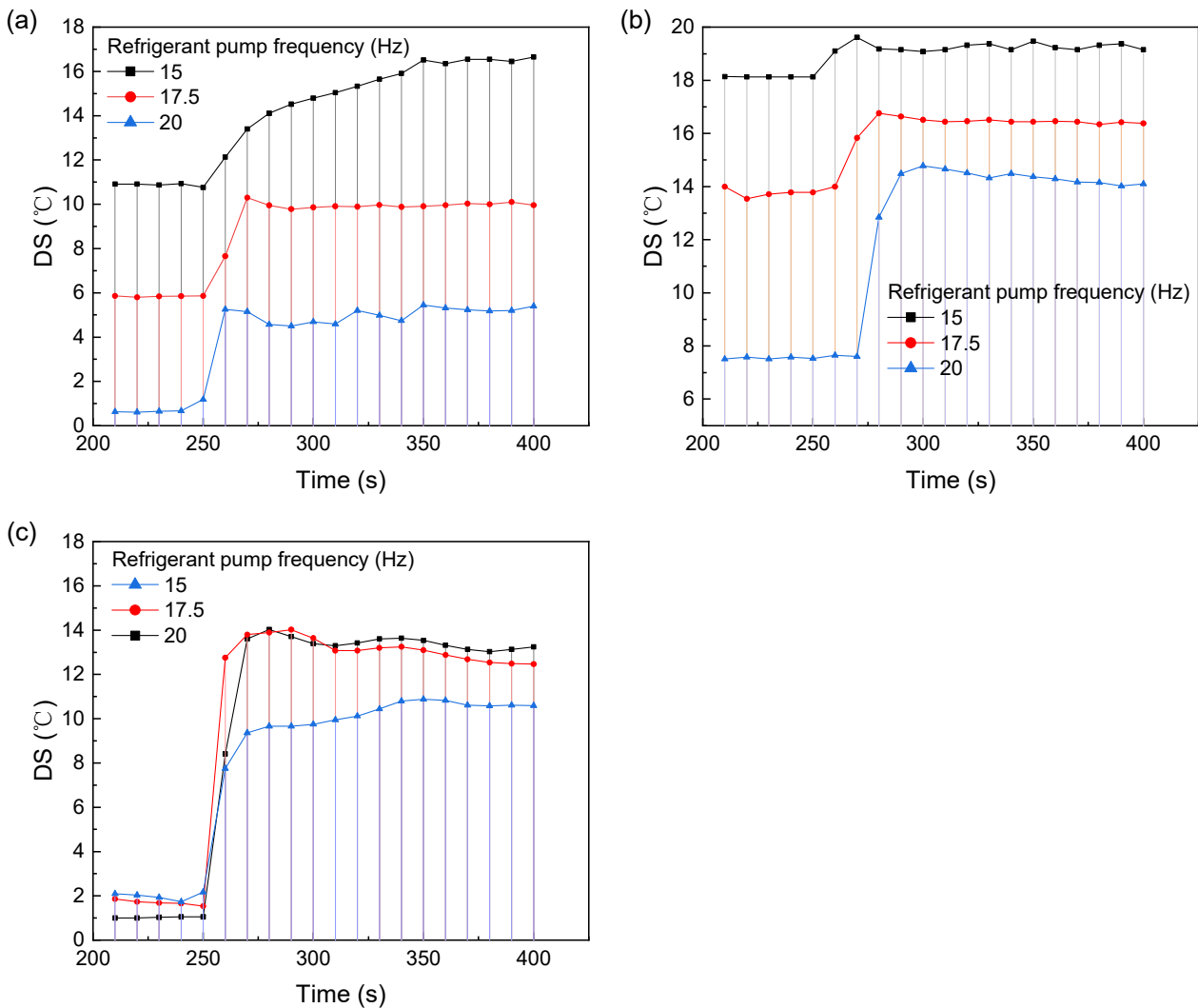
Figure 6. The change curves of DS when the EXV1 opening is adjusted from 30% to 10% (**a**) the refrigerant pump opening is 40%; (**b**) the refrigerant pump opening is 60%; (**c**) the refrigerant pump opening is 80%.

As can be seen from Figure 6, when the refrigerant pump opening is 40%, 60%, and 80%, the refrigerant pump frequencies corresponding to the fast response of the DS and its early stabilization time are 20 Hz, 17.5 Hz, and 15 Hz, respectively. Therefore, these three sets of data are selected for the self-tuning, as shown in Figure 7.

According to Figure 7 and the empirical formula of Ziegler-Nichols [36], the characteristic parameters of the DS, as well as the corresponding proportional adjustment coefficients K_p and integration time constants T_i of the PI control algorithm, can be derived under different conditions, as shown in Table 5.
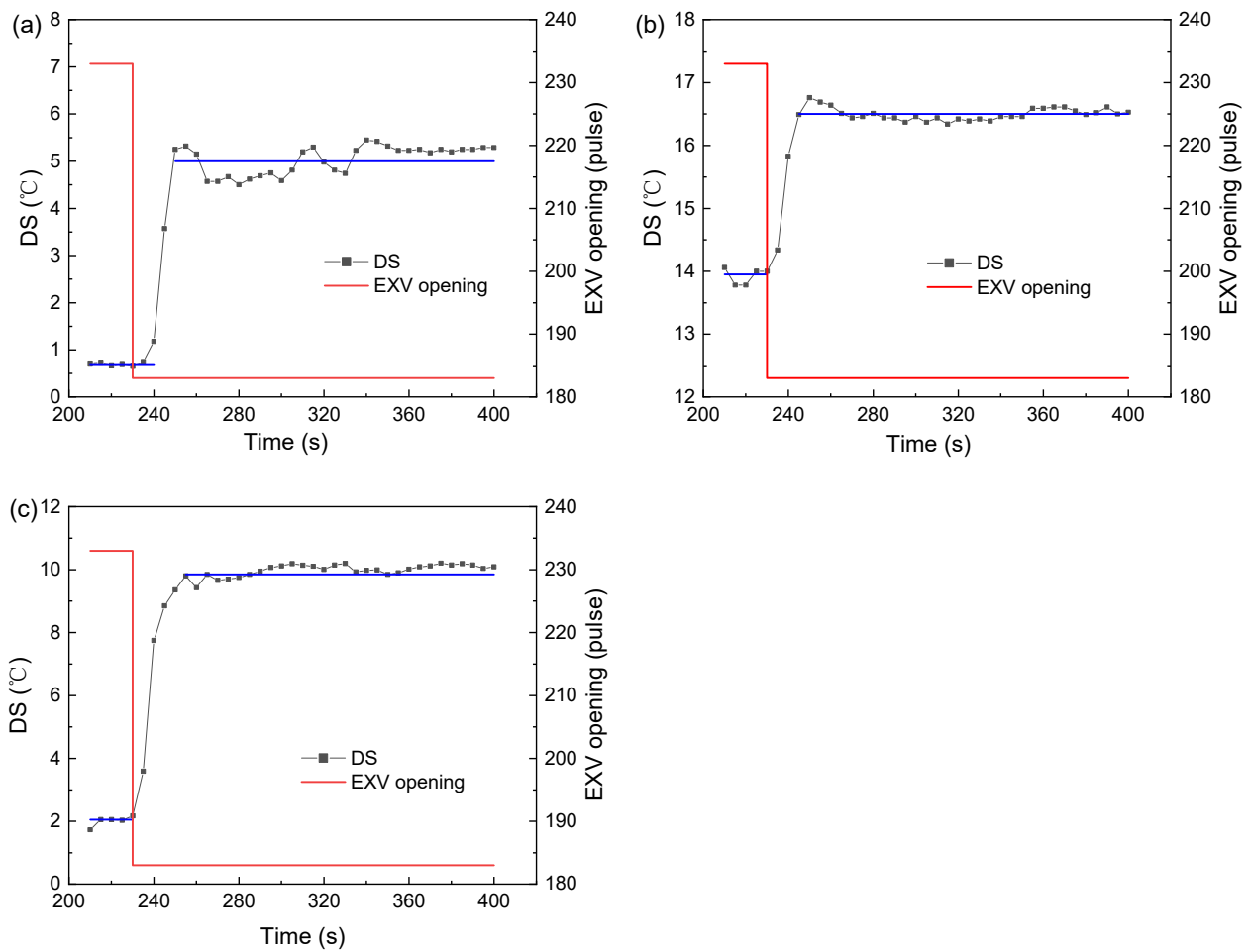
Figure 7. Response curves (**a**) refrigerant pump opening is 40%, frequency is 20 Hz; (**b**) refrigerant pump opening is 60%, frequency is 17.5 Hz; (**c**) refrigerant pump opening is 80%, frequency is 15 Hz.

Table 5. Parameters under different conditions.

Refrigerant Pump Opening (%)	Refrigerant Pump Frequency (Hz)	Characteristic Parameters			K_p	T_i
		k_1 (°C/pulse)	T_1 (s)	τ (s)		
40	20	−0.12	10	8	9.16	26.64
60	17.5	−0.06	7	8	12.9	26.64
80	15	−0.17	25	8	16.26	26.64

4.3. PI Control

The opening of EXV1 and EXV2 is first controlled by manual control to make the DS at the outlet of the test section reach the target value. The experimental conditions of EXV1 are that the opening and frequency of the refrigerant pump are 40% and 20 Hz, respectively, T3 is 23 °C, and T7 is −5 °C. The experimental conditions of EXV2 are that the opening and frequency of the refrigerant pump are 40% and 20 Hz, respectively, T3 is 23, 28, 33, 38 and 43 °C, and T7 is −5 °C. The manual control uses the dichotomous method to control the EXV opening to achieve the target value setting, and the curves of T3, T2, P1 and T_e are shown in Figure 8a,b when the DS is controlled by EXV2 and T3 is 23, 28 and 33 °C, respectively. The response curves of T3, T2, P1 and T_e at T3 is 38 and 43 °C, respectively, are shown in Figure 8c,d.

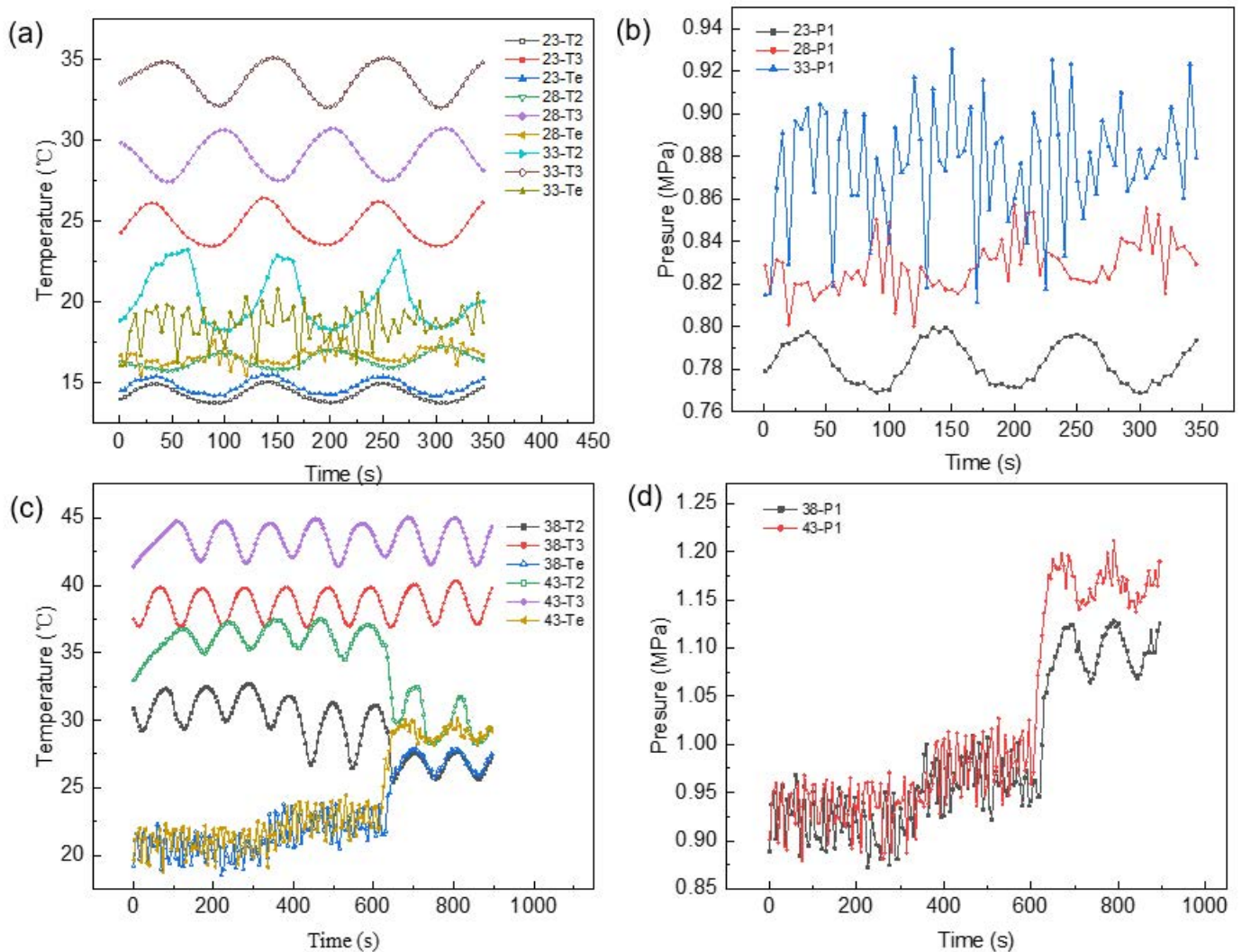**Figure 8.** Manual control of the EXV2 curves and response curves (**a**) the curves of T3, T2 and T_e when T3 is 23, 28 and 33 °C (**b**) the curves of P1 when T3 is 23, 28 and 33 °C; (**c**) the response curves of T3, T2 and T_e when T3 is 38 and 43 °C; (**d**) the response curves of P1 when T3 is 38 and 43 °C.

From Figure 8a,b, it can be seen that P1 increases with T3, and T_e increases with P1 and is higher than T2, indicating that the refrigerant in the test section is liquid. From Figure 8c,d, it can be seen that when T3 is set to 38 °C, during the process of the EXV2 opening is changed from 100% to 96%, P1 gradually increases, T_e rises with P1, and the refrigerant in the test section changes from the gaseous state to the gas-liquid two-phase state. Therefore, at lower temperatures, EXV2 is not suitable to be used for control of the test section outlet DS. In addition, it can be seen from Figure 8c,d that when the temperature of T3 is set to 43 °C, T_e gradually rises with the increase in P1 but is still lower than T2, and the refrigerant in the test section is gaseous, indicating that the control of the test section outlet DS by EXV2 can be achieved when T3 is 43 °C. Furthermore, the manual control effect of EXV2 is compared with EXV1, as shown in Figure 9.
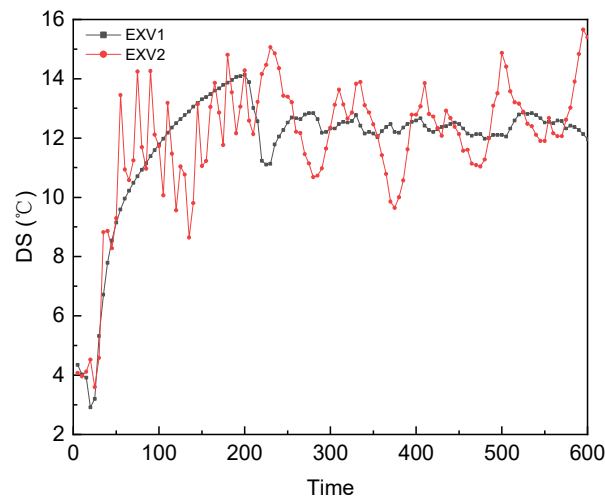
Figure 9. Manual control response curves.

From Figure 9, it can be seen that the overshoot of EXV1 is smaller and takes less time to stabilize compared to EXV2. Additionally, it needs electric heating to provide higher temperature and consume more energy when using EXV2 to control DS. Moreover, it can be seen from Figure 8d that with the change in EXV2 opening, the value of P1 is too large and even exceeds the safety pressure value set by the protection program. Therefore, EXV1 is selected for the control of the DS.

To realize the control of PI control algorithm, the designed algorithm is programmed into programmable logic controllers control program and uploaded to the control cabinet. Subsequently, under the same experimental conditions, the PI control algorithm was used to control the opening of EXV1, as shown in Figure 10a. It can be seen that the overshoot and fluctuations are larger. Therefore, the dichotomous and bilinear interpolation methods are used for optimization, as shown in Figure 10b.
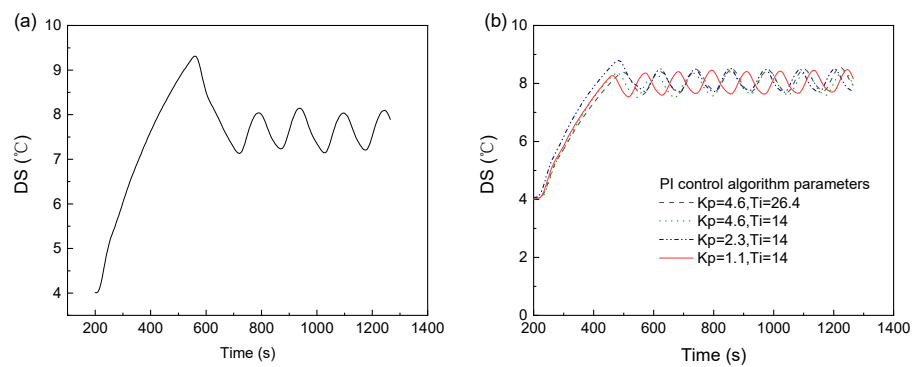

Figure 10. Response curves of PI cnotrol: (**a**) EXV1; (**b**) PI control parameters optimization.

It can be seen from Figure 10b that the optimized PI control algorithm parameters can achieve good control of EXV1, and the parameters are Kp = 1.1 and Ti = 14. Therefore, the same experimental debugging can be performed when the refrigerant pump opening is 60% and 80%. As shown in Figure 11, it is the response curve of the EXV1 manual and PI control DS. It can be seen that in the actual manual control process, the response is slow, the debugging process is long and fluctuates due to the presence of human factors. The PI control can respond more quickly and with less overshoot, i.e., with a maximum overshoot of 5.8% compared to manual control.
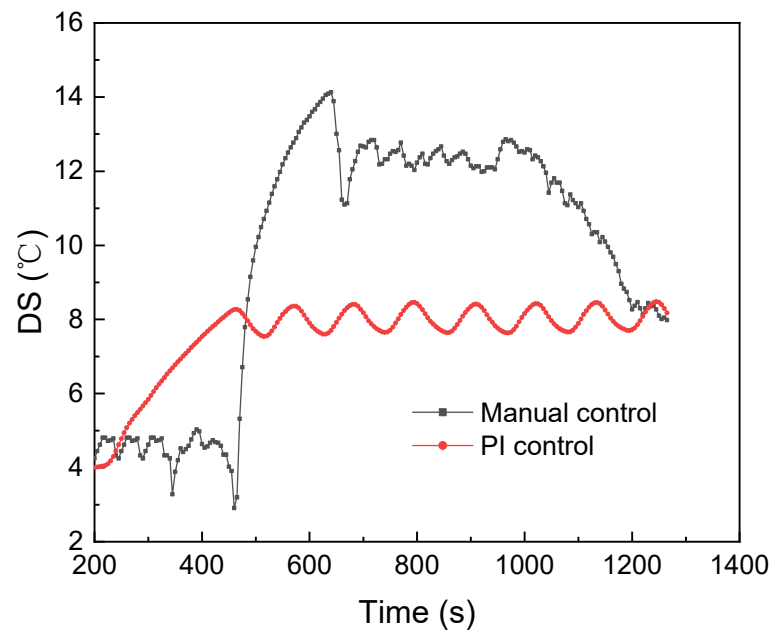
Figure 11. Manual and PI control DS response curves of EXV1, refrigerant pump opening is 60%.

In summary, a complete experimental system debugging solution can be obtained. The solution identifies the functional parameter settings and the PI control that is more efficient and convenient compared to manual control before achieving the control capability of EXV. By using the solution, the setting and debugging of similar experimental systems can be completed more efficiently, thereby improving the efficiency of the experimental process.

5. Conclusions

In this paper, from setting functional parameters of EXV to implementing the PI control, an experimental system debugging solution is obtained. The main conclusions are as follows:

(1) The effective opening range of the EXV of the experimental platform was obtained from 10% to 30% by conducting experiments under different operating conditions by manual control. Additionally, the control effects of EXV at different positions were analyzed. It is concluded that the EXV1 at the front end of the test section can better control the DS at the outlet of the test section and make the DS reach the target value.

(2) The PI control algorithm was used to control the EXV of the experimental platform. By optimizing the parameters after self-tuning, the PI control of the DS at the outlet of the test section is achieved. Compared with manual control, PI control can respond more quickly and with less overshoot, and its maximum overshoot is 5.8%.

(3) Using the experimental system debugging solution to conduct experiments cannot only reduce the time consumed by the experiment but also ensure the stability of the system and the accuracy of the experimental data. Moreover, because of the universality of the solution, it can be applied to the debugging of more experimental systems.

Author Contributions: Writing—original draft preparation, W.C.; calculation and data curation, J.W.; writing—review and editing, J.X. All authors have read and agreed to the published version of the manuscript.

Institutional Review Board Statement: Not applicable.

Nomenclature

$e(t)$	control algorithm input
$e(n)$	deviation value at the nth moment
DS	degree of superheat
EXV	electronic expansion valve
$G(s)$	transfer function
k_1	test section gain
K_i	integral coefficient of the control algorithm
K_p	proportional coefficient of the control algorithm
n	functional parameters, control serial number
n03	EXV model
n09	DS upper limit
n10	DS lower limit
n32	max opening
n37	number of steps from 0–100% opening
n38	number of steps per second
o	functional parameters
o10	signal type of external analog quantity
o18	manual control
o20	pressure sensor lower limit
o21	pressure sensor upper limit
o30	refrigerant type
o45	valve opening control
o56	control type
o61	external signal control
P	pressure (atm, MPa)
P1	test section outlet pressure (atm, MPa)
PI	proportional integral
s	Laplace operator
T	temperature (°C, K)
T_1	time constant
T1	test section inlet refrigerant temperature °C
T2	Test section outlet refrigerant temperature °C
T3	test section inlet water temperature °C
T7	Plate heat exchanger 3 inlet water temperature °C
T_e	evaporation temperature °C
T_i	integration time of the control algorithm
$u(t)$	control algorithm output
$u(n)$	control volume at the nth moment
τ	lag time
Subscripts	
1	state point
e	evaporation
i	integral
p	proportional

References

1. Knabben, F.T.; Ronzoni, A.F.; Hermes, C.J.L. Application of electronic expansion valves in domestic refrigerators. *Int. J. Refrig.* **2020**, *119*, 227–237. [CrossRef]
2. García del Valle, J.; Quinatoa Quinatoa, K.J.; Castro Ruiz, F. Experimental study of the static and dynamic behavior of a novel heat driven electronic controlled expansion valve. *Appl. Therm. Eng.* **2020**, *168*, 114718. [CrossRef]
3. Guo, J.; Jiang, F.M. A novel electric vehicle thermal management system based on cooling and heating of batteries by refrigerant. *Energy Convers. Manag.* **2021**, *237*, 114145. [CrossRef]
4. Li, R.; Zhu, Y.; Yang, Y.; Li, K.; Zhang, R.; Sun, J.; Sun, Z. The effects of the opening of the electronic expansion valve in the high-stage cycle on the performance of a cascade heat pump water heater. *J. Build. Eng.* **2021**, *42*, 103015. [CrossRef]
5. Zhang, R.; Stanke, E.J.; Zhang, G.; Lu, Y.; Sun, X.; Li, X. Benefits investigation of electronic expansion valve in electric vehicle thermal system as compared to thermal expansion valve with shut-off valve. *Int. J. Refrig.* **2019**, *100*, 404–413. [CrossRef]
6. Faegh, M.; Shafii, M.B. Thermal performance assessment of an evaporative condenser-based combined heat pump and humidification-dehumidification desalination system. *Desalination* **2020**, *496*, 114733. [CrossRef]
7. Wang, Y.; Ye, Z.; Song, Y.; Yin, X.; Cao, F. Experimental analysis of reverse cycle defrosting and control strategy optimization for transcritical carbon dioxide heat pump water heater. *Appl. Therm. Eng.* **2021**, *183*, 116213. [CrossRef]
8. Chen, Y.Y.; Zou, H.M.; Dong, J.Q.; Wu, J.; Xu, H.B.; Tian, C.Q. Experimental investigation on the heating performance of a CO_2 heat pump system with intermediate cooling for electric vehicles. *Appl. Therm. Eng.* **2021**, *182*, 116039. [CrossRef]
9. Park, C.; Cho, H.H.; Lee, Y.T.; Kim, Y.C. Mass flow characteristics and empirical modeling of R22 and R410A flowing through electronic expansion valves. *Int. J. Refrig. Rev. Int. Du Froid* **2007**, *30*, 1401–1407. [CrossRef]
10. Wang, Z.H.; Wang, F.H.; Ma, Z.J.; Song, M.J.; Fan, W.K. Experimental performance analysis and evaluation of a novel frost-free air source heat pump system. *Energy Build.* **2018**, *175*, 69–77. [CrossRef]
11. Knabben, F.T.; Melo, C.; Hermes, C.J.L. A study of flow characteristics of electronic expansion valves for household refrigeration applications. *Int. J. Refrig.* **2020**, *113*, 1–9. [CrossRef]
12. Liu, C.; Hou, Y.; Ma, J.; Liu, X.; Chen, L. Experimental study on the CO_2 flow characteristics through electronic expansion valves in heat pump. *Int. J. Refrig.* **2016**, *69*, 106–113. [CrossRef]
13. Chen, T.; Bae, K.J.; Kwon, O.K. Empirical correlation development of R245fa flow in electronic expansion valves. *Int. J. Refrig. Rev. Int. Du Froid* **2018**, *88*, 284–290. [CrossRef]
14. Beghi, A.; Cecchinato, L. A simulation environment for dry-expansion evaporators with application to the design of autotuning control algorithms for electronic expansion valves. *Int. J. Refrig. Rev. Int. Du Froid* **2009**, *32*, 1765–1775. [CrossRef]
15. Isler, Y.; Sahin, S.; Ekren, O.; Guzelis, C. Design of microcontroller-based decentralized controller board to drive chiller systems using PID and fuzzy logic algorithms. *Proc. Inst. Mech. Eng. Part E-J. Process Mech. Eng.* **2020**, *234*, 98–107. [CrossRef]
16. Wan, H.L.; Cao, T.; Hwang, Y.; Oh, S. An electronic expansion valve modeling framework development using artificial neural network: A case study on VRF systems. *Int. J. Refrig. Rev. Int. Du Froid* **2019**, *107*, 114–127. [CrossRef]
17. Kim, J.G.; Han, C.H.; Jeong, S.K. Robust Control for Variable Speed Refrigeration System Using a Disturbance Observer Based on H Optimization. *Korea J. Air-Cond. Refrig. Eng.* **2019**, *31*, 193–205. [CrossRef]
18. Zhiyan, M.; Lei, Y.; Min, S.; Xukang, Z. Small cold storage monitoring system based on LabVIEW. *Food Ind.* **2020**, *41*, 248–252.
19. Xia, Y.; Deng, S. The influences of the operating characteristics of an Electronic Expansion Valve (EEV) on the operational stability of an EEV controlled direct expansion air conditioning system. *Int. J. Refrig.* **2016**, *69*, 394–406. [CrossRef]
20. Ding, X.; Wang, J.; Duan, P.; Yin, C.; Zhang, F. A novel on-line auto-tuning PI controller for the superheat of evaporator with electronic expansion valve. In Proceedings of the 2017 Chinese Automation Congress (CAC), Jinan, China, 20–22 October 2017; pp. 7513–7517.
21. Taler, D.; Sobota, T.; Jaremkiewicz, M.; Taler, J. Influence of the Thermometer Inertia on the Quality of Temperature Control in a Hot Liquid Tank Heated with Electric Energy. *Energies* **2020**, *13*, 4039. [CrossRef]
22. Al-Badri, A.R.; Al-Hassani, A.H. A control method using adaptive setting of electronic expansion valve for water chiller systems equipped with variable speed compressors. *Int. J. Refrig.* **2020**, *119*, 102–109. [CrossRef]
23. Taler, D.; Sobota, T.; Jaremkiewicz, M.; Taler, J. Control of the temperature in the hot liquid tank by using a digital PID controller considering the random errors of the thermometer indications. *Energy* **2022**, *239*, 122771. [CrossRef]
24. Cruz, G.G.; Mendes, M.A.A.; Pereira, J.M.C.; Santos, H.; Nikulin, A.; Moita, A.S. Experimental and numerical characterization of single-phase pressure drop and heat transfer enhancement in helical corrugated tubes. *Int. J. Heat Mass Transf.* **2021**, *179*, 121632. [CrossRef]
25. Shah, M.M. A general correlation for heat transfer during evaporation of falling films on single horizontal plain tubes. *Int. J. Refrig.* **2021**, *130*, 424–433. [CrossRef]
26. Aroonrat, K.; Ahn, H.S.; Jerng, D.-W.; Asirvatham, L.G.; Dalkılıç, A.S.; Mahian, O.; Wongwises, S. Experimental study on evaporative heat transfer and pressure drop of R-134a in a horizontal dimpled tube. *Int. J. Heat Mass Transf.* **2019**, *144*, 118688. [CrossRef]
27. Diani, A.; Brunello, P.; Rossetto, L. R513A condensation heat transfer inside tubes: Microfin tube vs. smooth tube. *Int. J. Heat Mass Transf.* **2020**, *152*, 119472. [CrossRef]
28. Wang, D.; Tian, R.; Li, L.; Dai, X.; Shi, L. Heat transfer of R134a in a horizontal internally ribbed tube and in a smooth tube under super critical pressure. *Appl. Therm. Eng.* **2020**, *173*, 115208. [CrossRef]

29. Jige, D.; Kikuchi, S.; Mikajiri, N.; Inoue, N. Flow boiling heat transfer of zeotropic mixture R1234yf/R32 inside a horizontal multiport tube. *Int. J. Refrig.* **2020**, *119*, 390–400. [CrossRef]

30. Copetti, J.B.; Macagnan, M.H.; Zinani, F. Experimental study on R-600a boiling in 2.6 mm tube. *Int. J. Refrig.* **2013**, *36*, 325–334. [CrossRef]

31. Enoki, K.; Ono, M.; Okawa, T.; Kristiawan, B.; Wijayanta, A.T. Water flow boiling heat transfer in vertical minichannel. *Exp. Therm. Fluid Sci.* **2020**, *117*, 110147. [CrossRef]

32. Chang, W.; Xie, J.; Wang, J.; Teng, W.; Sun, Y.; Zheng, M. Application of PLC and HMI in the measurement and control platform of single-tube heat transfer experiment rig. *Adv. Mech. Eng.* **2020**, *12*, 168781402097116. [CrossRef]

33. Chang, W.Y.; Wang, J.F.; Xie, J.; Teng, W.Q. Investigation on Switchable Evaporation and Condensation Horizontal Single Tube Heat Exchange Experiment Platform. In *IOP Conference Series: Earth and Environmental Science*; IOP Publishing: Bristol, UK, 2021; Volume 701, p. 012061. [CrossRef]

34. Danfoss. *Data Sheet Electronic Expansion Valves Type ETS 6*; Danfoss: Nordborg, Denmark, 2013.

35. Aprea, C.; Renno, C. Experimental analysis of a transfer function for an air cooled evaporator. *Appl. Therm. Eng.* **2001**, *21*, 481–493. [CrossRef]

36. Ziegler, J.G.; Nichols, N.B. Optimum Settings for Automatic Controllers. *Trans. ASME* **1942**, *64*, 759–768. [CrossRef]